Compact, passively *Q*-switched Nd:YAG laser for the MESSENGER mission to Mercury

Danny J. Krebs, Anne-Marie Novo-Gradac, Steven X. Li, Steven J. Lindauer, Robert S. Afzal, and Anthony W. Yu

A compact, passively *Q*-switched Nd:YAG laser has been developed for the Mercury Laser Altimeter, an instrument on the Mercury Surface, Space Environment, Geochemistry, and Ranging mission to the planet Mercury. The laser achieves 5.4% efficiency with a near-diffraction-limited beam. It passed all space-flight environmental tests at subsystem, instrument, and satellite integration testing and successfully completes a postlaunch aliveness check en route to Mercury. The laser design draws on a heritage of previous laser altimetry missions, specifically the Ice Cloud and Elevation Satellite and the Mars Global Surveyor, but incorporates thermal management features unique to the requirements of an orbit of the planet Mercury.

OCIS codes: 140.3480, 120.2830.

1. Introduction

The Mercury Surface, Space Environment, Geochemistry, and Ranging (MESSENGER) mission to the planet Mercury requires a laser altimeter capable of performing range measurements to the surface of the planet over highly variable distances and with a constantly changing thermal environment.[1–3] Specifically the satellite will execute an orbit with a periapsis of 200 km and an apoapsis of approximately 15,200 km, with an orbital period of 12 h. For the altimeter instrument, science observations are taken during the 0.5 h of closest approach to the planet. The laser must support the instrument requirement of achieving a range resolution of less than 40 cm to the surface of the planet. The anticipated radiation exposure over the mission life is 30 krad (Si), total dose, assuming an effective shielding of 0.1 cm of aluminum.[4] During the close approach to the day side of the planet the satellite is heating, and it is not possible to fully isolate the laser subsystem from the rest of the satellite. In terms of laser performance it is necessary to achieve more than 18 mJ of output energy in a near-diffraction-limited beam with ~6-ns pulses at an 8-Hz repetition rate, while the laser bench temperature is executing a thermal ramp from 15 to 25 °C at a rate of approximately 0.4 °C/min.

2. Description of the Laser

To satisfy the requirements above, we chose an oscillator/amplifier architecture with passive *Q* switching (see Fig. 1). This approach is similar to one taken by the Geoscience Laser Altimeter System[5] (GLAS) laser instrument, previously developed by NASA for the Ice Cloud and Elevation Satellite mission. The primary difference between this laser and the lasers in the GLAS instrument is that only one amplifier slab is used in this laser, whereas the GLAS lasers have two stages of amplification. The oscillator/amplifier approach has several advantages for this application: (1) The saturated loss of the passive *Q* switch affects only the efficiency of the oscillator section, thereby enabling a reasonable overall efficiency with a passive *Q* switch. (2) The small mode diameter (~0.1 cm) of the oscillator permits a compact and stable laser resonator with reasonable alignment tolerance. (3) The ratio of internal to external optical fluence is lessened relative to the oscillator-only systems.

The oscillator section comprises a crossed-porro optical resonator[6–8] with polarization output coupling, a Brewster's angle Nd:Cr:YAG slab pumped by a sin-

All authors are affiliated with NASA Goddard Space Flight Center, Greenbelt, Maryland 20771. S. Lindauer is with Northrop Grumman Laser Systems, 2787 South Orange Blossom Trail, Apopka, Florida 32703. R. Afzal is with Spectra Systems Corporation, 321 South Main Street, Providence, Rhode Island 02903. A. Yu is with Northrop Grumman Electronic Systems, 1745 West Nursery Road, MS1155, Linthicum, Maryland 21090.

Received 4 August 2004; revised manuscript received 16 November 2004; accepted 19 November 2004.

0003-6935/05/091715-04$15.00/0

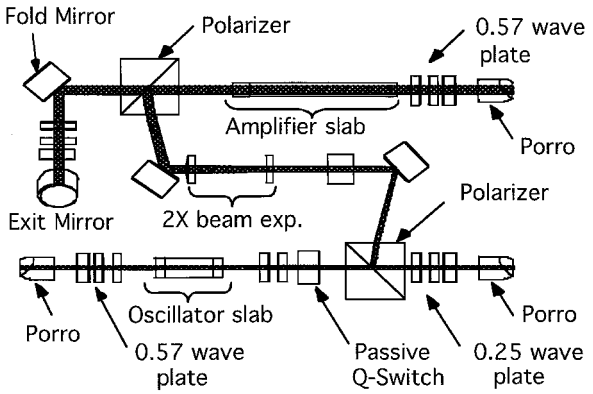

Fig. 1. Optical layout of the MLA laser.

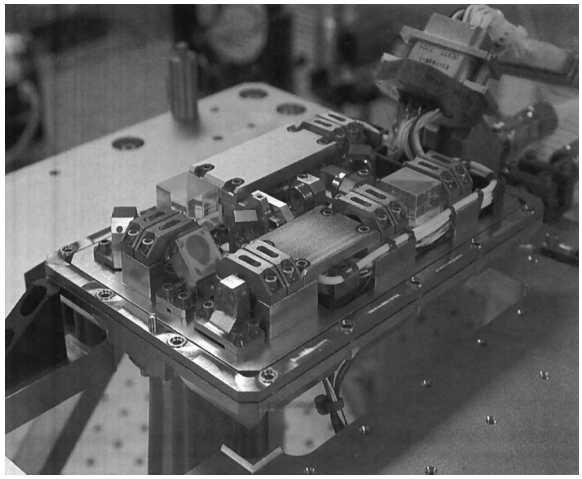

Fig. 2. View of the laser bench.

gle two-bar stack of GaInAsP laser diode bars (Coherent G-2), an air gap polarizer (Synoptics), a passive Q switch (Cr^{4+}, 0.46 optical density, Scientific Materials Inc.), zero-order quartz wave plates for polarization control, and fused-silica Risley wedges for optical alignment. A thermoelectric cooler is employed between the pump array and the laser bench to keep the oscillator pump array at its design temperature and output wavelength. The (0.5%) Cr^{3+} codoping of the Nd:Cr:YAG slab enhances the resistance of that element to radiation darkening.[9] The nominal oscillator mode diameter is 1.0 mm, and its output energy is 3.0 mJ in a 5-ns pulse. The physical length of the oscillator is 10.8 cm. The cavity Q was adjusted by rotating the angle of the quarter-wave plate to produce the Q-switched laser pulses after 0.15 ms of pumping.

The oscillator output beam undergoes a (2× magnification) beam expansion and is amplified 8.7 dB by a Nd:Cr:YAG amplifier slab. The slab is double-passed with the first pass p polarized with respect to the Brewster endfaces and the second pass s polarized with respect to the endfaces. The input and output faces of the slab are coated to achieve low loss in both p and s polarizations. The amplifier slab is pumped by two, four-bar stacks of GaInAsP laser diode bars (Coherent G-4). The pump arrays for the oscillator and the amplifier sections are operated in series, electrically, driven at a 100-A peak current. As described in detail below the laser electronics terminates the laser diode drive pulse once a Q-switched laser output pulse is detected. The isolation of the amplifier output beam from its input beam is accomplished by polarization. A 0.57-retardation wave plate together with the porro-prism reflector provides a polarization change in the backreflected beam to the orthogonal linear polarization. Size and weight constraints preclude use of a Faraday isolator. Because the isolation level achieved with this approach is only approximately −17 dB, we found it necessary to offset the pointing of the input and output beams of the amplifier so that the backreflected amplified spontaneous emission from the amplifier does not overlap the oscillator mode in the Q switch.

Overlap results in the premature bleaching of the passive Q switch and lessening of the output energy. We used beam stops in key locations to intercept backreflected energy. Unlike the oscillator pump array there is no direct control of the amplifier pump array temperature. Therefore the output wavelength and pumping efficiency of the amplifier pump arrays vary with the optical bench temperature.

A (15× magnification) beam expander[10] is mounted to the underside of, and perpendicular to, the laser optical bench. A quarter-wave plate between the beam expander and the laser prevents backreflected energy from external optics from entering the amplifier. The output polarization of the laser subsystem is therefore circular. On the backside of the optical mount for the exit mirror, i.e., the mirror that directs the output beam to the 15× beam expander, we attached a diffuser plate to intercept the leakage through the exit mirror. A quadrant photodiode (UDT Sensors, SPOT-4D) staring at this diffuser plate provides (1) a timing signal for terminating the laser diode pump pulse, (2) laser energy monitoring, and (3) a start signal for the ranging electronics. To provide a greater signal level for the critical function of triggering the ranging system, the signals from three quadrants of the detector are summed to provide the ranging start signal. The remaining quadrant of the detector provides the signal for terminating the laser pumps and energy monitoring. The laser electronics is designed to provide a maximum laser diode drive pulse of 0.24-ms duration. As configured the oscillator Q switches at 0.15 ms, and the signal from the quadrant photodiode terminates the laser diode drive pulse at that time. As the laser ages the time to fire increases. The pump duration capacity of the electronics provides an approximate 35% specific gain margin to accommodate the pump array degradation and additional resonator losses at end of life.

The mechanical design of the laser utilizes a beryllium optical bench (9.27 cm × 14.1 cm × 1.1 cm) for reduced mass and enhanced thermal performance (Fig. 2). A titanium spacer is used to optimize the

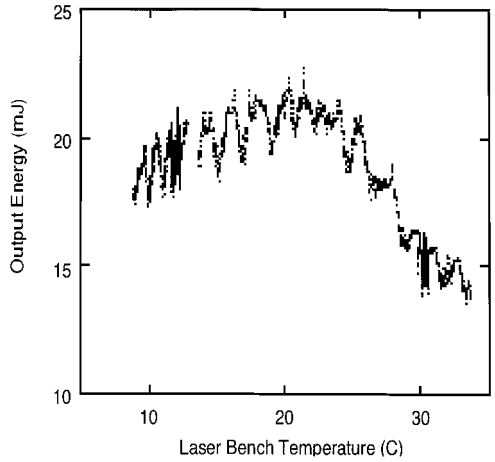

Fig. 3. Laser output energy versus bench temperature, measured in vacuum.

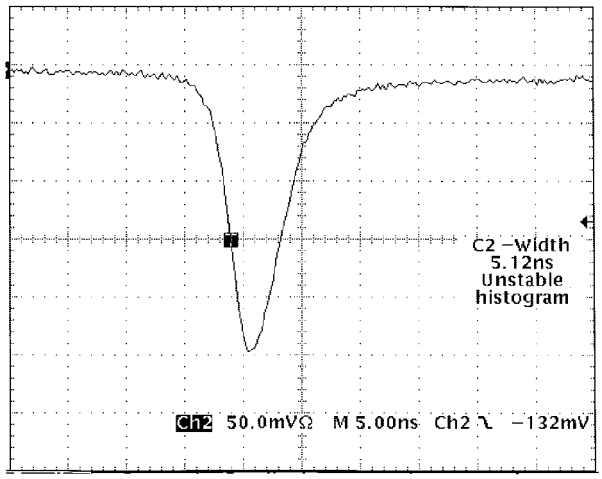

Fig. 4. Laser pulse temporal profile. Horizontal scale, 5 ns.

thermal isolation of the laser bench from the rest of the instrument subsystem, and a small heater ensures that the laser bench starts each science observation period at a temperature of 15 °C. The weight allocations of 0.52 kg for the laser and 0.32 kg for the laser electronics are satisfied.

3. Performance of the Laser Subsystem

The environmental tests of the laser subsystem consisted of vibration and thermal vacuum testing. Vibration testing consisted of three-axis random vibration to a rms of 8.0 g in x and y, and a rms of 10.7 g in z, with a full evaluation of the laser pointing, power, and divergence before and after each test.

The thermal-vacuum testing involved a nonoperational warm soak at 40 °C, a nonoperational cold soak at 5 °C, followed by a cold start, a hot start at 35 °C, and four operational thermal sweep cycles, all in vacuum conditions. During this testing the output power, divergence, beam pointing, and pointing stability were measured continually. A 4-m, focal-length, off-axis parabola was employed in the evaluation of beam pointing and divergence. The baseline for beam-pointing measurements was provided by the normal-incidence reflection of a collimated He–Ne beam off a reference mirror bonded to the base of the laser bench. We independently verified that the reference mirror axis was aligned to the mechanical axis of the laser bench to within approximately 20 μrad. In instrument level testing a coalignment stability of 7 μrad rms between the transmitted laser beam and the receiver system was measured.[4] The wavelength was measured at each stabilized temperature with a Burleigh pulsed wave meter.

Figure 3 shows the output energy of the laser subsystem over a temperature sweep between 10 and 35 °C. The overall shape of the curve is due to changes in the output wavelength of the amplifier pump array and consequent changes in absorption efficiency. We believe that the (0.8–1.5 °C) periodicity of the data is related to the Fabry–Perot resonances of the oscillator.

Figure 4 shows the laser pulse temporal profile. We observed no mode beating in the large majority of pulses.

The laser maintained a stable TEM_{00} spatial mode over the entire range of the thermal sweep (Fig. 5). The best Gaussian-fit divergence was 75 μrad (~1.67 times the diffraction limit). Encircled energy measurements revealed that there was approximately 25% energy outside the 75-μrad Gaussian core (compared with an ideal of 13.6%). The nonideal character of the encircled energy was not fundamental to the design and probably could have been corrected with additional work. It was decided, however, to accept this level of beam quality as entirely satisfactory for meeting the measurement requirements of the mission.

The receiver system[10] incorporates a spectral filter with a 0.7-nm (FWHM) bandwidth. To ensure system performance over the full operating temperature of the laser bench, it was important to verify laser wavelength stability. The laser output wavelength was measured to be sufficiently stable against changes in bench temperature (Fig. 6) that it will not be a factor in the performance over the temperature of the ranging system. The pulse width of the laser was in the

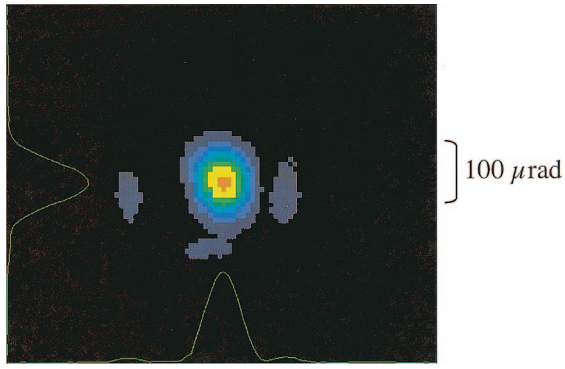

Fig. 5. Laser output mode.

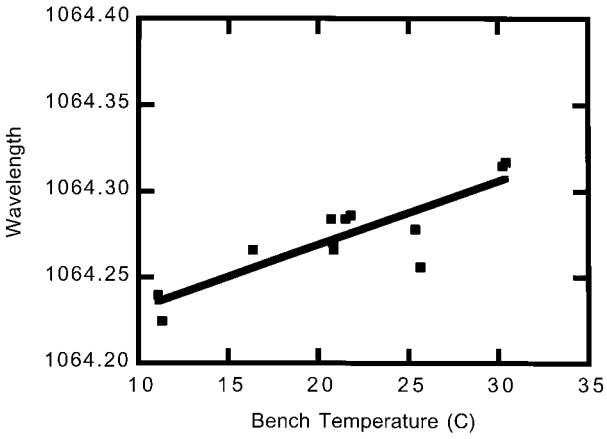

Fig. 6. Laser output wavelength versus bench temperature.

range of 4.6–5.0 ns and was quite stable. The overall efficiency of the laser subsystem, including the electronics, thermoelectric cooler, and quadrant detector, was 2.8%. The efficiency of the laser head (optical energy out divided by electrical energy into the diode arrays and the thermo-electric cooler) was 5.4%. In instrument level tests the overall ranging system achieved a single-shot resolution of 0.4 ns, corresponding to a range resolution of 6 cm.[4] The anticipated ranging accuracy is 12 cm rms.

4. Conclusion

We have reported on a highly compact and lightweight laser source for ranging applications in space missions. The laser meets its key requirements for output energy, beam quality, pulse width, pointing stability, and wavelength.

The authors acknowledge the support of the Mercury Laser Altimeter Science Team, especially David E. Smith, the principal investigator. This research benefited from the contributions of dozens of individuals at NASA and among our suppliers, so any list of contributors is inadequate. We particularly acknowledge the efforts of Jeff Guzek (mechanical design), Jamie Britt (mechanical lead), Luis Nagao (assembly), Robert Taminelli (facilities), Linda Miner (optics), F. David Robinson (optics test), Israel Moya (mechnical), Paul Haney (optics bonding), Alberto Rosanova (parts processing), Mark Stephen (laser diode qualification), Alexander Vasilyev (laser diode test), Randy Hedgeland (contamination), Xiaoli Sun (instrument analysis), Jeremy Karsh (quadrant detector), James Smith (systems engineer), John Canham (contamination), Luis Ramos-Izquierdo (optics design), Keith Corsi (quality assurance), Kevin Novo-Gradac (contamination), Edward Amatucci (project management), and Arlin Bartels (project management). They provided outstanding support in their respective roles.

References

1. S. C. Solomon, R. L. McNutt, Jr., R. E. Gold, M. H. Acuna, D. N. Baker, W. V. Boynton, C. R. Chapman, A. F. Cheng, G. Gloeckler, J. W. Head III, S. M. Krimigis, W. E. McClintock, S. L. Murchie, S. J. Peale, R. J. Phillips, M. S. Robinson, J. A. Slavin, D. E. Smith, R. G. Strom, J. I. Trombka, and M. T. Zuber, "The MESSENGER mission to Mercury: scientific objective and implementation," Planet. Space Sci. **49,** 1445–1465 (2001).
2. R. E. Gold, S. C. Solomon, R. L. McNutt, Jr., A. G. Santo, J. B. Abshire, M. H. Acuna, R. S. Afzal, B. J. Anderson, G. B. Andrews, P. D. Bedini, J. Cain, A. F. Cheng, L. G. Evans, W. C. Feldman, R. B. Follas, G. Gloeckler, J. O. Goldsten, S. E. Hawkins III, N. R. Izenberg, S. E. Jaskulek, E. A. Ketchum, M. R. Lankton, D. A. Lohr, B. H. Mauk, W. E. McClintock, S. L. Murchie, C. E. Schlemm II, D. E. Smith, R. D. Starr, and T. H. Zurbuchen, "The MESSENGER mission to Mercury: scientific payload," Planet. Space Sci. **49,** 1467–1479 (2001).
3. A. G. Santo, R. E. Gold, R. L. McNutt, Jr., S. C. Solomon, C. J. Ercol, R. W. Farquhar, T. J. Hartka, J. E. Jenkins, J. V. McAdams, L. E. Mosher, D. F. Persons, D. W. Artis, R. S. Bokulic, R. F. Conde, G. Dakermanji, M. E. Goss, Jr., D. R. Haley, K. J. Heeres, R. H. Maurer, R. C. Moore, E. H. Rodberg, T. G. Stern, S. R. Wiley, B. G. Williams, C. L. Yen, and M. R. Peterson, "The MESSENGER mission to Mercury: spacecraft and mission design," Planet. Space Sci. **49,** 1481–1500 (2001).
4. X. Sun, J. F. Cavanaugh, J. C. Smith, and A. E. Bartels, "Design and performance measurement of the Mercury Laser Altimeter," in *Technical Digest, 2004 Conference on Lasers and Electro-optics*, on CDE-ROM (The Optical Society of America, Washington, D.C., 2004), presentation CThN3.
5. J. B. Abshire, J. C. Smith, and B. E. Schutz, "The Geoscience Laser Altimeter System," in Technical Digest, 19th International Laser Radar Conference, Annapolis, Md., NASA Conference Rep. CP-1998-207671 (NASA, Greenbelt, Md., 1998).
6. R. S. Afzal, "The Mars Observer Laser Altimeter: laser transmitter," Appl. Opt. **33,** 3184–3188 (1994).
7. G. Zhou and L. W. Casperson, "Modes of a laser resonator with a retroreflecting roof mirror," Appl. Opt. **20,** 3542–3546 (1981).
8. R. S. Afzal, A. W. Yu, J. J. Zayhowski, and T. Y. Fan, "Single-mode, high-peak-power, passively *Q*-switched, diode-pumped Nd:YAG laser," Opt. Lett. **22,** 1314–1316 (1997).
9. T. S. Rose, M. S. Hopkins, and R. A. Fields, "Characterization and control of gamma and proton radiation effects on the performance of Nd:YAG and Nd:YLF lasers," IEEE J. Quantum Electron. **31,** 1593–1602 (1995).
10. L. Ramos-Izquierdo, V. S. Scott III, S. Schmidt, J. Britt, W. Mamakos, R. Trunzo, J. Cavanaugh, and R. Miller, "Optical system design and integration of the Mercury Laser Altimeter," Appl. Opt. **44,** 1748–1760 (in this issue).